Electronic Supplementary Material (ESI) for Chemical Communications

Effect of Gas Pressure on Negative Thermal Expansion in MOF-5

Nina Lock[1], Mogens Christensen[1], Cameron J. Kepert[2] and Bo B. Iversen[1]*

[1]Center for Materials Crystallography, Department of Chemistry and iNANO, Langelandsgade 140, DK-8000 Aarhus C, Denmark

[2]School of Chemistry, The University of Sydney, Sydney NSW 2006, Australia

*Corresponding author: bo@chem.au.dk

Experimental Details and Comments

Synthesis: MOF-5 was synthesized by the previously reported solvothermal approach using $Zn(NO_3)_2 \cdot 6H_2O$ and 1,4-benzenecarboxylic acid as precursors.[1] The solvent was removed from the synthesized MOF-5 crystals under dynamic vacuum, and the resulting solvent-free cubic single crystals were stored in argon atmosphere.

Multi-temperature synchrotron powder X-ray diffraction at low gas pressure: A powder of MOF-5 was loaded into a polyimide (Kapton) capillary with an inner diameter of 0.85 mm in an argon filled glove bag. The capillary was mounted in a sample cell[2] available at the Advanced Photon Source (APS), Argonne National Laboratory, USA. The cell was purged with helium gas for 1 hour at room temperature to exchange argon in the capillary with helium. A cap was mounted on the cell to keep the sample at a constant helium overpressure of 0.7 bar. Powder X-ray diffraction data were collected using a wavelength of 0.62 Å at the 1-BM beamline at the APS. The exact wavelength was determined from a NIST LaB_6 standard. An Oxford Cryostream was used to control the sample temperature. The sample was initially cooled to 100 K, and data were collected continuously in the temperature range 100-500 K on a MAR-345 image plate detector while heating the sample at a rate of 120 K/h. The exposure time was 12.0 seconds per frame.

In situ multi-temperature synchrotron powder X-ray diffraction at high gas pressures: A MOF-5 powder was filled into a 0.4 mm glass capillary in an argon glovebox. The glass capillary was placed in a single crystal sapphire tube with an inner diameter of 0.75 mm. Ferrules, Swagelok fittings and epoxy made a seal to the sapphire tube, which can withstand pressures of more than 150 bar. Helium pressures were applied directly to the sample from a standard helium cylinder. The pressure was controlled from outside the experimental hutch, where the gas cylinder equipped with standard regulators, Swagelok tubing and a proportional relieve valve (PRV) was installed. The PRV was used to release overpressure from the system, and the sapphire cell was mounted on a goniometer. The setup is sketched in Figure S1. The sapphire tubes, ferrules, Swagelok fittings, and PRV are parts of a reactor designed to perform *in situ* powder diffraction studies of hydrothermal reactions; this reactor is described in detail elsewhere.[3] The inert gas in the sapphire cell effectively consists of a helium/argon mixture, since the sapphire tube was loaded in an argon glovebox and thus contains argon at ambient pressure. Helium was chosen for pressurizing the cell, as this gas was used as pressure medium in the INS study.[4] However, even at the lowest pressure of 5 bar, helium is present in a much larger concentration than argon. Only the sapphire tube itself initially contained argon at ambient pressure, as all Swagelok tubing was purged with helium prior to applying the pressure. Nevertheless, the argon residue may slightly influence the gas adsorption (especially at 5 bar), as gaseous impurities were previously found to influence H_2 adsorption in MOF-5.[5]

Synchrotron radiation powder diffraction data were collected at MAX-lab, Lund, Sweden at the wiggler beam line I711 using a wavelength of 1.00 Å. A LaB_6 standard from NIST was used for calibration. An exposure time of 12.0 s per frame was used, and a MarCCD 165 detector measured the diffracted intensities. The sample was cooled using an Oxford Instruments Cryojet liquid nitrogen cooler. The cryojet uses a constant gas flow to cool the sample rather than cooling at a certain controllable rate. Data collection was initiated at room temperature and powder patterns were measured continuously while the sample was cooled. A flow rate of 6 L/min N_2 was used to cool the sample to a set temperature of 130 K. At a temperature of approximately 140 K the sample was heated to 150 K, equilibrated and subsequently cooled at an increased cooling gas rate of 9 L/min to a set temperature of 100 K. All multi-temperature data series at 5, 50, 100, and 150 bar were collected using identical cooling profiles. Due to the relatively thick walls of the capillary tubes, the *actual* sample temperature in the sapphire capillary during cooling was found to be higher than the temperature displayed on the cryojet controller (see also the discussion in the manuscript).

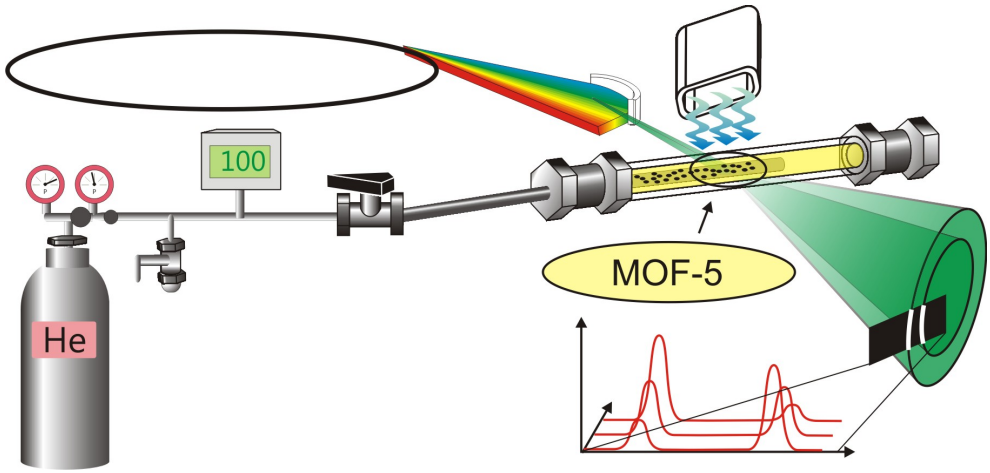

Figure S1. Sketch of the setup used for the experiments at 5-150 bar. MOF-5 powder was packed into a glass capillary which was loaded into a single crystalline sapphire tube. A helium gas pressure was applied on the sample directly from a helium cylinder using standard regulators. Data were collected continuously as the sample was cooled. A proportional relieve valve was used to remove the pressure from the system.

Data analysis: All 2D data frames were integrated using the program Fit2D.[6] A few intense single crystal sapphire Bragg reflections were masked from the high pressure data prior to integration. Low pressure data were Le Bail fitted using the Fullprof software.[7] A Thomson-Cox Hastings pseudo-Voigt function was used for profile fitting, and the background was described by linear interpolation. The high pressure data were Rietveld refined sequentially in Fullprof. A simple model which did not take gas atoms into account was applied. The zero point was refined for one data set and fixed for all data series to avoid correlation between zero point and cell parameter. The Gaussian and Lorenzian profile parameters, *U* and *X*, were

refined for one dataset and fixed. The *B*-overall parameter was fixed to a value of -1.0, a value which is not physical sound, but which resulted in better fits than by using a constant positive value. The reason for this is a systematic error, likely absorption by the sapphire tube. The value of *B* does not influence the determination of the cell parameter, which is focus in this study. The scale factor, cell parameter, the Gaussian profile parameters *W* and *V* were refined along with 8 background points and the *x*-coordinate of the Zn-atom.

Powder Diffraction Data

The high pressure data at 5 bar and 150 bar are very weak due to a partial loss of the synchrotron ring current after data collection of the 50 and 100 bar experiments. Figure S2a shows the first data set (at room temperature) from the high pressure experiments. Figure S2b shows the refined powder diagram at room temperature and 50 bar. The corresponding refinement parameters are shown in Table S1.

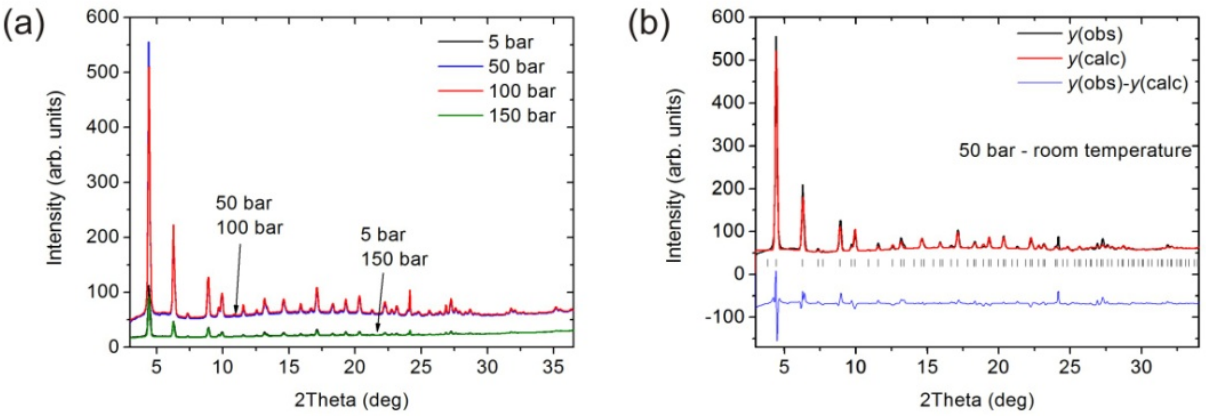

Figure S2. (a) The first powder diagram at room temperature from the 5, 50, 100, and 150 bar experiments (collected at identical exposure times) revealing that the synchrotron ring current decreased after the 50 and 100 bar experiments had been carried out. (b) The room temperature data at 50 bar is shown as an example of a refined powder diagram.

Table S1. Refinement parameters and results corresponding to data displayed in Figure S2b. The *R*-values are high, but the cell parameter, which is the most important parameter for this study, has a low uncertainty.

Refinement parameters			
Scale factor	$1.327(9)\cdot10^{-8}$	*U*	0.0085 (fixed)
a (Å)	25.756(1)	*V*	0.020(15)
x(Zn)	0.2063(4)	*W*	0.028(1)
R_B (%); R_F (%)	16.5; 19.6	*X*	0.0586 (fixed)
N(reflections)	131	*Y*	0.0 (fixed)
N(parameters)	13		

Temperature and Pressure Dependent Unit Cell

Figure S3 evidences the temperature off-set around 150 K exemplified by the 50 bar data.

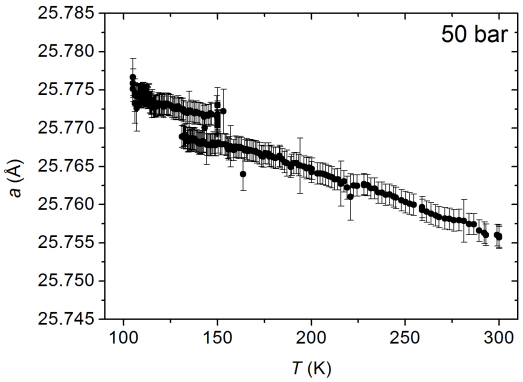

Figure S3. Temperature dependent unit cell revealing a difference between the actual temperature and the cryojet temperature. Therefore, data below 150 K are not considered further in this paper.

Figure S4 shows the unit cell as a function of temperature (150-300 K) for the 5, 50, 100, and 150 bar data during cooling (black circles) and during temperature equilibration (open red circles). Few outliers have been omitted.

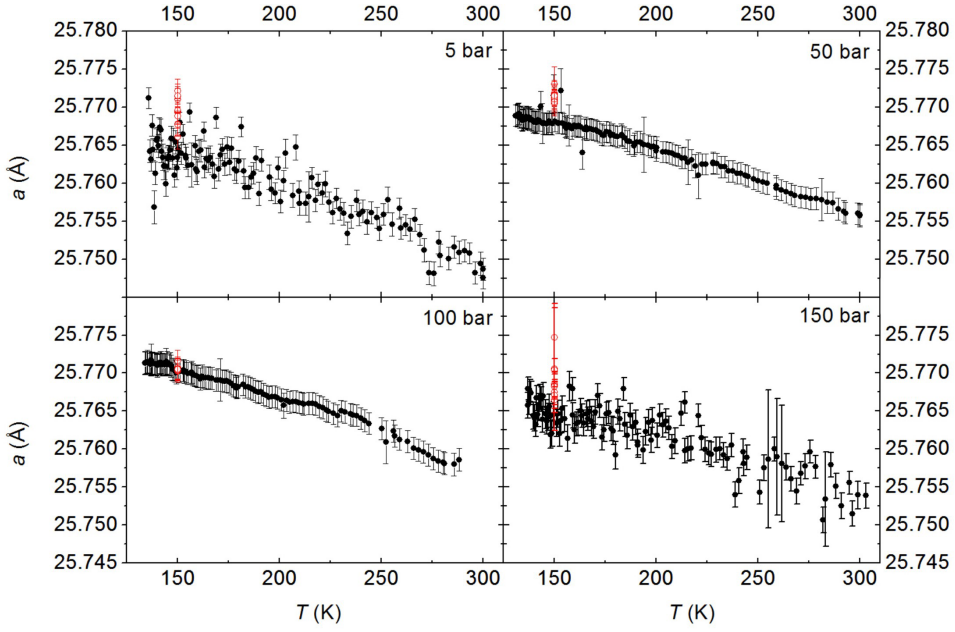

Figure S4. The MOF-5 unit cell as a function of pressure and temperature during cooling (filled black circles) and after temperature equilibration (open red circles). NTE is clearly maintained even at a pressure of 150 bar. The data collected at 5 bar and 150 bar are more scattered than the 50 and 100 bar data due to decreased data quality caused by a partial loss of the synchrotron current in the storage ring (Figure S2).

In Figure S5a all black data points (cooling) from Figure S4 were averaged three by three. Figure S5b shows a plot of data normalized to the unit cell parameter at 285 K. The thermal expansion behavior at the pressures of 5-150 bar are almost identical. The errors in Figure S5b are quite large (the average error is 0.00166 Å).

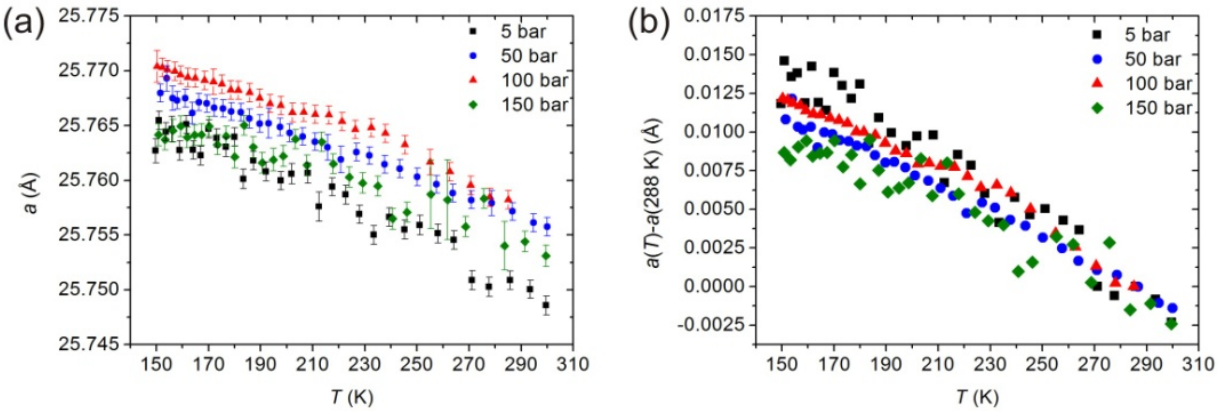

Figure S5. (a) Unit cell parameters in the 150-300 K range averaged three by three (corresponds to the manuscript Figure 2b). (b) The averaged unit cell parameters normalized to 285 K. The errors are not plotted for clarity, but the average error is 0.00166 Å.

Determination of the Coefficients of Thermal Expansion

Low Pressure

Figure S6 shows linear fits used to determine the CTE for the near-ambient pressure data using all data (100-500 K) and by using data in the 150-300 K range only.

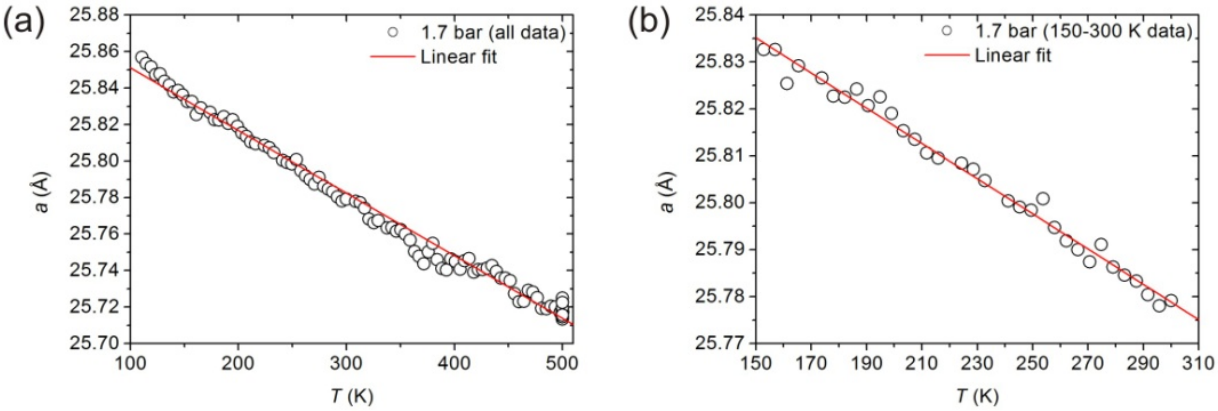

Figure S6. Linear fits to the near-ambient pressure data for (a) all data (100-500 K) and (b) data in the 150-300 K range for comparison with the high pressure data. The errors are smaller than the symbols and have not been plotted here.

High pressure

The near-room temperature and the equilibrated 150 K data were used for determination of CTEs for the 5-150 bar data by fitting linear curves to the data (Figure S7). Figure S8 evidences that thermal equilibrium had been reached at 150 K for the data which were used to determine the CTEs.

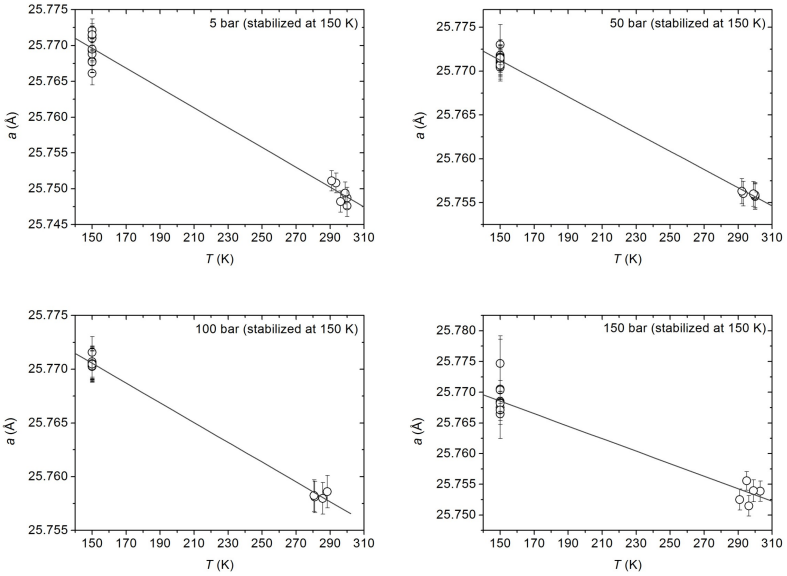

Figure S7. Determination of the linear CTE based on near-room temperature data and the 150 K data after thermal equilibration (non-averaged data).

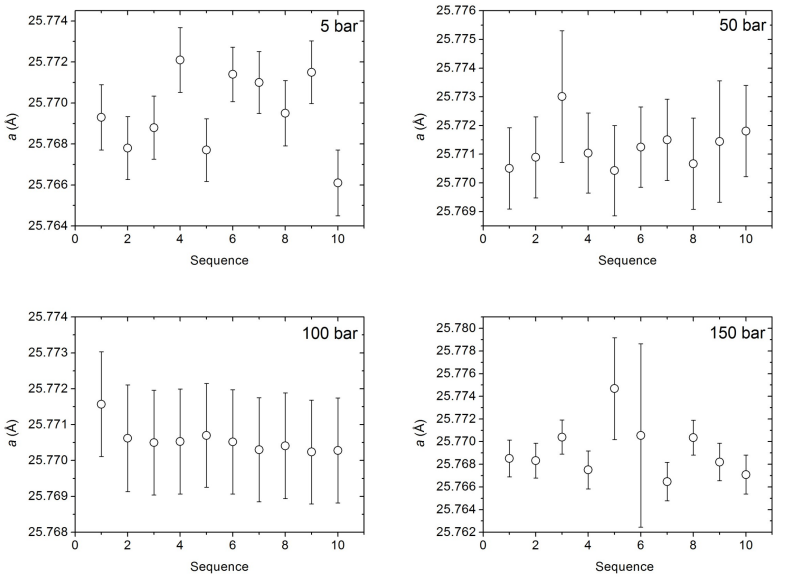

Figure S8. Unit cell of the temperature stabilized sample at 150 K plotted in the order in which they were collected. This reveals that the sample temperature was stable before resuming the data collection.

For comparison with the CTEs obtained from the fits shown in Figure S7, linear functions were fitted to all data in the 150-300 K range which were collected as the sample was cooled down (Figure S9).

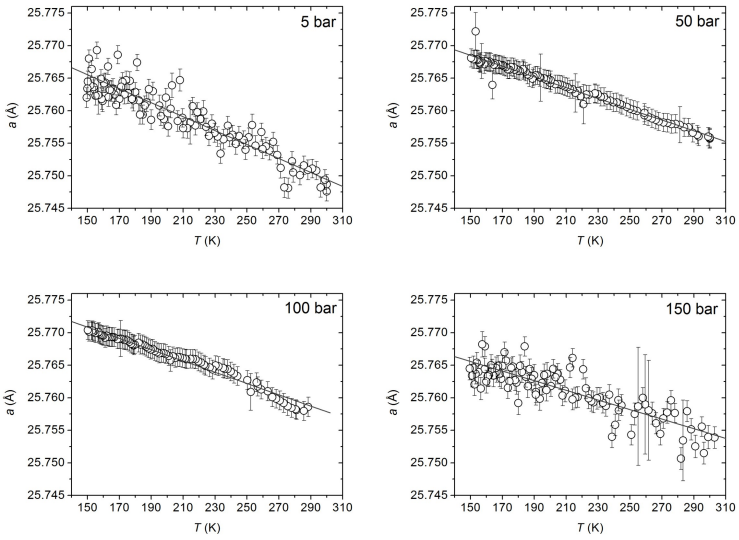

Figure S9. Linear fits to the unit cell parameters extracted from data collected when the sample was cooled down (excluding the data collected after temperature stabilization at 150 K). Linear fitting is reasonable at 5, 50, and 150 bar, but the 100 bar data seems to consist of two domains: 150-225 K and 225-288 K.

The CTEs for all experiments are shown in Figure S10 and Table S2. As expected there is a difference between the CTEs obtained from the temperature stabilized sample and the value based on all data. However, the trends are the same: NTE decreases by applying a pressure from 5 bar to 50 bar, whereas the effect of increasing the pressure above 50 bar is negligible. The values based on the thermally equilibrated data are considered the most reliable data.

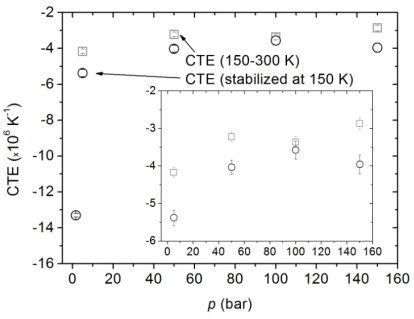

Figure S10. Linear CTEs at 288 K are plotted as a function of pressure. The black circles and grey squares are based on the linear fits displayed in Figure S7 and Figure S9, respectively. The inset only contains data points corresponding to the 5-50 bar experiments.

Table S2. Linear CTEs corresponding to the values shown in Figure S7 and Figure S9.

Linear Coefficient of Thermal Expansion		
Pressure (bar)	α_l(288 K) ($\cdot 10^6$ K^{-1}) (150 K and RT data – Figure S7)	α_l(288 K) ($\cdot 10^6$ K^{-1}) (all data 150-300K – Figure S9)
1.7	-13.3(1)*	---
5	-5.4(2)	-4.2(2)
50	-4.0(2)	-3.2(1)
100	-3.6(2)	-3.4(2)
150	-4.0(2)	-2.9(2)
*Based on data all data in the 150-300 K range (Figure S6).		

The large difference between the near ambient and 5 bar CTE may suggest that external (isotropic) pressure as well as internal pressure (adsorption) plays a role on the damping. Moreover, argon residues may to some extent influence adsorption properties (see Experimental Details in this ESI).

References

1 N. Lock, Y. Wu, M. Christensen, L. J. Cameron, V. K. Peterson, A. J. Bridgeman, C. J. Kepert and B. B. Iversen, *J. Phys. Chem. C,* 2010, **114,** 16181.

2 P. J. Chupas, K. W. Chapman, C. Kurtz, J. C. Hanson, P. L. Lee and C. P. Grey, *J. Appl. Cryst.,* 2008, **41,** 822.

3 J. Becker, M. Bremholm, C. Tyrsted, B. Pauw, K. M. Ø. Jensen, J. Eltzholtz, M. Christensen and B. B. Iversen, *J. Appl. Crystallogr.,* 2010, **43,** 729.

4 N. Lock, M. Christensen, Y. Wu, V. K. Peterson, M. K. Thomsen, A. J. Ramirez-Cuesta, G. J. McIntyre, K. Norén, R. Kutteh, C. J. Kepert, G. Kearley, and B. B. Iversen, *Dalton Trans,* 2012, DOI: 10.1039/C2DT31491F

5 J. L. C. Rowsell, A. R. Millward, K. S. Park, and O. M. Yaghi, *J. Am. Chem. Soc.* 2004, **126,** 5666.

6 A. P. Hammersley, S. O. Svensson, M. Hanfland, A. N. Fitch and D. Hausermann, *High Press. Res.,* 1996, **14,** 235.

7 J. Rodriguez-Carvajal, *Physica B,* 1993, **192,** 55.